

Systematically improvable optimized atomic basis sets for *ab initio* calculations

Mohan Chen,¹ G-C Guo,¹ and Lixin He ^{*1}

¹*Key Laboratory of Quantum Information,
University of Science and Technology of China,
Hefei, 230026, People's Republic of China*

(Dated: November 1, 2018)

Abstract

We propose a unique scheme to construct fully optimized atomic basis sets for density-functional calculations. The shapes of the radial functions are optimized by minimizing the *spillage* of the wave functions between the atomic orbital calculations and the converged plane wave calculations for dimer systems. The quality of the bases can be systematically improved by increasing the size of the bases within the same framework. The scheme is easy to implement and very flexible. We have done extensive tests of this scheme for wide variety of systems. The results show that the obtained atomic basis sets are very satisfactory for both accuracy and transferability.

PACS numbers: 71.15.Ap, 71.15.Mb

* corresponding author: helx@ustc.edu.cn

I. INTRODUCTION

The last few years have seen the development of the first-principles methods in the application of complex material systems containing hundreds and thousands of atoms.¹⁻⁴ This is made possible because of the so called linear scaling algorithms⁵ are used, by taking the advantages of the locality of the electronic structures.⁶ The widely used plane wave basis is not suitable for the linear scaling algorithms, because of its extended nature. Instead, the local basis, such as atomic orbitals are the better choices.

The advantage of atomic orbitals are two folds. First, the basis size of atomic orbitals is much smaller compared to other basis sets, such as plane wave, and real space mesh, etc. Second, the atomic orbitals are strictly localized and therefore compatible with the linear scaling algorithms⁵ for electronic calculations. However, the atomic basis sets must be constructed very carefully to ensure both good accuracy and transferability. Furthermore the quality of the basis sets should be systematically improvable in an unbiased way.

Several schemes to construct atomic orbitals have been proposed.^{2,7,8} For example, the atomic orbitals can be constructed by applying certain confinement potentials to the isolated atoms.^{9,10} To ensure the transferability of the orbitals, one could use larger basis set, by using more than one radial function for each angular moment (multi- ζ), or by including higher angular moment orbitals (polar orbitals). Empirically, the multi- ζ functions can be generated by split-valence method,⁷ whereas the polar orbitals can be generated by applying electric field in addition to the confinement potential. These methods have been demonstrated to be effective.⁷ Nevertheless, different level of orbitals are treated in different ways, and are not guaranteed to be the optimized ones.⁴ Volker *et al.* proposed a way to systematically improve the basis that they choose the one that improves the energy most from a large pool of *pre-selected* orbitals.² Alternatively, Ozaki optimize shape of atomic orbitals adopted to different environment as part of the self-consistency cycle.⁸ However, in this scheme, every atom must has different orbital shape even for the same element.

In this work, we propose a unique method that allows to construct systematically improvable fully optimized atomic basis sets for density-functional calculations. Unlike previous methods, all the orbitals (including multi- ζ and polar orbitals) can be constructed in a same procedure. The shapes of the radial functions are optimized by minimizing the *spillage* of the wave functions between the converged plane wave calculations and those from atomic

orbital calculations for dimer systems, and therefore no pre-assumption about the radial functions is needed. The scheme is easy to implement and is very flexible and efficient. We have done extensive tests of this scheme for wide variety of systems. The results are very promising, showing very satisfactory results for both accuracy and transferability.

The rest of paper is organized as follows. In Sec. II we give detailed introduction of our scheme to construct atomic orbitals. We test the obtained orbitals by calculating the structural and electronic properties of wide variety of systems in Sec. III, including III-V and group IV semiconductors, and GaN, ZnO, Al, Pb and MgO etc. We summarize in Sec. IV.

II. METHODS

One of the most popular ways to generate the atomic orbitals is to use atomic orbitals of isolated atoms in certain confinement potentials. This procedure usually gives the minima basis of the atom. To make the basis more complete, one has to use multi-zeta orbitals and polar orbitals. The multi-zeta orbitals can be obtained via a split-valence method,⁷ whereas the polar orbitals are generated by applying constant electric fields.⁷ Obviously, the orbitals are constructed in very different procedures. The quality of the orbitals are uncontrolled, even though they are usually good. When larger basis sets are needed for high quality calculations, the procedures to get the orbitals are tedious.

We use a very different strategy to construct fully optimized atomic orbitals that are highly transferable. The strategy is based on minimizing the spillage of the wave functions between the atomic orbital calculations and the plane wave results. The spillage is a measurement of the difference between the Hilbert space spanned by a set of local basis and the space spanned by the “exact” wave functions of the interested states of given systems.^{11,12} The spillage is defined as,¹¹

$$\mathcal{S} = \frac{1}{N_n} \sum_{n=1}^{N_n} \langle \Psi_n | 1 - \hat{P} | \Psi_n \rangle, \quad (1)$$

where Ψ_n is the plane wave calculated eigenstate and N_n is the number of states of interest. \hat{P} is a projector which spanned by all the atomic orbitals, i.e.,

$$\hat{P} = \sum_{\mu\nu} |\phi_\mu\rangle S_{\mu\nu}^{-1} \langle \phi_\nu|, \quad (2)$$

where $\phi_\mu = \phi_\mu(\mathbf{r} - \mathbf{r}_\mu)$ is the μ -th local orbital. $S_{\mu\nu}$ is the overlap matrix between orbitals ϕ_μ and ϕ_ν , i.e.,

$$S_{\mu\nu} = \langle \phi_\mu | \phi_\nu \rangle, \quad (3)$$

where $\mu = \{\alpha, i, \zeta, l, m\}$, in which α is the element type, i is the index of atom of each element type, ζ is the multiplicity of the radial functions for the angular momentum l , and m is the magnetic quantum number.

The spillage has been applied to analyze the quality of given atomic basis sets.¹¹⁻¹⁴ There are also some attempts to choose optimized local basis for a given system by minimizing the spillage value.¹¹⁻¹³ In these methods, it usually starts from certain pre-assumed orbital shapes with few free parameters. The spillage is then used to determine these parameters. In Ref. 12, the authors used the spillage to choose the best Slater-type orbitals or the pseudo atomic orbitals for a given system. However, the transferability of the atomic orbitals are not taken into consideration. Using similar idea, Kenny *et al.* took one step further and generated multi- ζ and polar orbitals.¹³

Here we propose a new scheme based on the spillage formalism to generate high quality atomic orbitals that are systematically improvable. Our method improves upon that of previous methods in three aspects: (i) The shape of atomic orbitals can be generated automatically without any pre-assumptions. (ii) The atomic basis can be systematically improved within the same framework. (iii) The transferability of the atomic bases is improved by carefully choosing the reference systems.

1. The radial functions

In our scheme, each atomic orbital is written as a radial function multiplied by a spherical harmonic function. The radial functions are expanded into spherical Bessel functions. The μ -th local orbital is $\phi_\mu(\mathbf{r}) = f_{\mu,l}(\mathbf{r})Y_{lm}(\hat{r})$, where,

$$f_{\mu,l}(\mathbf{r}) = \begin{cases} \sum_q c_{\mu q} j_l(qr), & r < r_c \\ 0 & r \geq r_c. \end{cases} \quad (4)$$

$j_l(qr)$ is the spherical Bessel function. q is chosen to satisfy $j_l(qr_c)=0$, where r_c is the cut off radius of the radial functions. The atomic orbitals are therefore strictly zero beyond r_c . $Y_{lm}(\hat{r})$ is the spherical harmonic function, in which l is the angular momentum, m is the

magnetic quantum number. The coefficients $c_{\mu q}$ are chosen to minimize the spillage of the reference systems via a simulated annealing method. Since the first-principles total energy calculation can be done once for all for the reference system, the method is very efficient.

We use the same energy cutoff of plane wave calculation for the spherical Bessel functions. For pseudopotentials calculations, 15 ~ 30 spherical Bessel functions are usually good enough to obtain reliable atomic orbitals.

In order to make the kinetic energy integral well defined, one needs to make the second derivative of the atomic orbitals continuous. This can be done by multiplying the radial part of the atomic orbitals by a smooth function,¹³

$$g(r) = 1 - \exp\left[-\frac{(r - r_{\text{cut}})^2}{2\sigma^2}\right]. \quad (5)$$

In our test, we find σ has little influence on the final results, we thus fix $\sigma=0.1$.

In our scheme, we do not have to assume the shape of the atomic orbitals, therefore in principle we can get the fully optimized radial functions.

2. Reference systems

One first needs to generate the atomic basis sets for some reference systems, then use it to more general cases, assuming the atomic basis sets are transferable. A good reference system is therefore crucial for generating high quality transferable basis set. Here, we choose dimer systems as reference systems. The spillage of the system is defined to be the average spillage values of the few selected dimers.² We choose several dimers at different bonding lengths, covering the whole dissociate curve of the dimer. If only one dimer is used as the reference, it will leave a finger print into the atomic orbitals, therefore worsen their transferability. We find 4 or 5 dimers are enough to generate reliable local orbitals. Further increasing the number of dimers to the reference system as many as 20 does not significantly improve the results. As it will be shown in the paper, the atomic basis generated from the dimer systems can be used to calculate different bulk systems with high accuracy, showing remarkable transferability. This is very important for studying complex material system, which may have complex chemical environment in a single system, including defects, surfaces, alloy etc.

3. Systematically generate atomic orbitals

The quality of the numerical orbital basis set can be systematically improved by increasing the number of radial functions (multi-zeta orbitals) of given angular momentum and by including orbitals with higher angular momentum (polar orbitals). There are several ways in the literature to construct multi-zeta orbitals and polar orbitals. However, there is still no systematically way to generate multi-zeta orbitals and polar orbitals, in which all orbitals are treated in a unbiased way.⁴ In contrast, in our scheme all orbitals can be generated with the same procedures. To do so, we first generate the orbitals with given angular momentum, which we can call level 1 orbitals. The higher level orbitals can be generated using the same procedure, by minimize the spillage of the remaining Hilbert space, which orthogonal to the space spanned by the all previously generated atomic orbitals. Taken Si DZP (i.e., double ζ functions plus one polar orbitals basis as an example. In the first step, we generate the first s and p orbitals, which form a minimal basis set for Si. In the second step, we generate the second s and p orbitals (multi-zeta orbitals). We first orthogonalize the wave functions of the reference states to the atomic orbitals generated in step 1. Here we define the projector operator formed by level 1 orbitals as,

$$\hat{P}^{(1)} = \sum_{\mu\nu} |\phi_{\mu}^{(1)}\rangle S_{\mu\nu}^{-1} \langle\phi_{\nu}^{(1)}| \quad (6)$$

where $\phi_{\mu}^{(1)}$ is the μ -th orbital of level 1 orbitals. The remaining wave functions are,

$$|\Psi_n^{(2)}\rangle = (1 - \hat{P}^{(1)})|\Psi_n^{(1)}\rangle \quad (7)$$

where $|\Psi_n^{(2)}\rangle$ is the new set of wave functions, which is orthogonal to the atomic orbitals generated at step 1, i.e.,

$$\hat{P}^{(1)}|\Psi_n^{(2)}\rangle = 0. \quad (8)$$

We then minimize the spillage between the second s , p orbitals and the space spanned by $|\Psi_n^{(2)}\rangle$. In step 3, we generate the d orbitals following exactly the same procedures. The order of the orbitlas added into the basis can be determined by choosing the orbitals that decrease the spillage most after the orbitals have been added to the basis. In such way, we can systemtically generate orbitals of any multiplicity and angular momentum in a unified scheme. This is important if high accuracy calculations are needed.

4. Optimize the shape

To give an idea of how the obtained radial functions look like using the above scheme, we show the radial functions of the first 3 s , p , d atomic orbitals in Fig. 1 (a), (b), (c) respectively for the carbon atom. The orbitals are obtained by taking five carbon dimers of different bond lengths as reference systems. The bond length of the dimmers are chosen to be 1.00, 1.25, 1.50, 2.00, 2.50 Å. The energy cutoff of plane wave basis calculations is set to 100 Ry. The radius cutoff r_c is chosen to be 6 a.u.. As we can see, the radial functions of these atomic orbitals have many oscillations. These oscillations are unphysical and may lower the transferability of the atomic basis set. To get rid of the alloying oscillations of the orbitals, at each step after we obtain the orbitals which minimize the spillage, we add a procedure to optimize the shape of the radial functions as follows. We define the “kinetic energy” of an atomic orbital as,

$$T_\mu(c_{\mu q}) = \sum_q c_{\mu q}^2 q^2 / 2 + \kappa, \quad (9)$$

where q satisfy $j_l(qr_c)=0$. $c_{\mu q}$ are the coefficients of the spherical Bessel functions that normalize the atomic orbitals, i.e., $\langle \phi_\mu | \phi_\mu \rangle = 1$. κ is a penalty function that

$$\kappa = \begin{cases} 0, & \mathcal{S}/\mathcal{S}_0 - 1 < \Delta \\ \infty, & \mathcal{S}/\mathcal{S}_0 - 1 > \Delta \end{cases}, \quad (10)$$

where \mathcal{S}_0 is the minimal spillage value for the given orbital set, and \mathcal{S} is the current spillage value for the given coefficients $c_{\mu q}$. We found $\Delta=0.002 \sim 0.005$ can be sufficient to smooth out the atomic orbitals. The “kinetic energies” of the atomic orbitals are also minimized via a simulated annealing method. After the shape optimization, the final spillage values will be slightly larger than the minimal ones, and have little influence on the accuracy of these basis sets.

The shape optimized orbitals are plotted in Fig.1 (d), (e), (f), for the s , p , d orbitals respectively, compared to those of unoptimized orbitals. As we see the alloying oscillations in the original orbitals have been gotten rid of, and the shapes of the optimized orbitals are much smoother than the origin ones, which implies a better transferability. We calculate the total energies of the reference dimmers using the optimized orbitals and find that they offer the same accuracy for the selected dimmers as the origin ones.

III. RESULTS AND DISCUSSION

In this section, we do intensive tests on the accuracy and transferability of the atomic orbital basis sets generated using the the scheme given in Sec. II for wide variety of materials, including covalent, ionic, metallic systems. The lattice constants, bulk modulus, band structures calculated from the atomic basis are compared to those calculated from plane wave basis. Especially, GaN, ZnO and Al are known to have several stable structures that are energetically very close to each other, which provide very good tests on the quality of the atomic basis sets.

All the calculations were done using density functional methods^{15,16} (DFT) with local density approximation(LDA) in Perdew-Zunger form.¹⁷ Norm conserving pseudopotentials¹⁸ are used in fully separate form.¹⁹ Periodic boundary condition is used for solids systems, and the integration over Brillouin zone is replaced by sum up Monkhorst-Pack k points.²⁰

A. Cutoff radii of orbitals

The range of radial function r_c is one of the most important parameters of the atomic orbitals. Usually larger r_c leads to more accurate results, but at the same time demands more computational time and memory. One needs to choose proper r_c that balance the two factors. For 3D solid, the number of neighboring atoms increases very fast as r_c^3 , one has to use modest r_c , whereas for 2D and 1D systems, r_c can be relatively larger. It is also important to balance the errors of different elements in the system.²¹ As one shall see below, it is straightforward to use the spillage value as a criterion to choose a proper r_c for each element. Using the silicon diamond structure as an example. The energy cutoff is chosen to be 50 Ry and the k points are chosen to be $6 \times 6 \times 6$, which are enough to converge the total energies. In Fig.2 the blue curve is the total energy difference between the Si DZP basis and the plane wave calculations, whereas the red curve is the spillage, as a function of r_c . As we see that both the spillage value and the total energy decrease monotonically as r_c increases and are almost on top of each other. When $r_c=6$ a.u., the energy difference can be reduced to about 1.5 eV per unit cell, and decreases rapidly to about 0.25 eV per unit cell at $r_c=8$ a.u.. The spillage values for these two r_c are about 9×10^{-3} and 2×10^{-3} , respectively. Tests on other elements show similar results, which clearly demonstrate that

the spillage is an excellent criterion for the quality of the atomic basis set.

In order to further show how r_c affects the spillage, we show in Fig.3 (a),(b) the spillage of different basis size changes with r_c for Si and C diamond structures. As we see, if r_c is too small, further increasing the size of the basis does not significantly improve the quality of basis. For example, for Si dimers, if one chose $r_c=7$ a.u., DZP basis has spillage about 3.5×10^{-3} , further increasing the basis size does not lower the spillage too much. However, increasing r_c will dramatically decrease the spillage. For $r_c=12$ a.u., the spillage value of DZP basis can be as small as 8×10^{-4} . Figure 3(b) shows similar results for diamond. However, as it is shown in the figure, carbon DZP orbitals with $r_c=6$ a.u. are as good as DZP orbitals of silicon with $r_c=8$ a.u.. The lesson we can learn from the tests is that one should choose proper basis set size for a given r_c .

B. III-V and group IV semiconductors

Semiconductors are a class of important materials. Here we test our atomic bases for III-V and group IV semiconductors. The energy cutoff is chosen to be 50 Ry and the k points are chosen as $6\times 6\times 6$, unless otherwise noticed. The results are summarized in Table I. The r_c of Ga, In, Al, As, P, Sb, Ge elements are chosen to be 9 a.u. whereas r_c of silicon and carbon is chosen to be 8 a.u. and 6 a.u., respectively. We use plane wave basis results as benchmark, also listed in Table I. We can see that the results from the single-zeta (SZ) basis (the minimal basis) have large deviations for both lattice constants and bulk modulus. SZ basis predict too large lattice constants than those calculated from plane wave basis for more than 0.1 -0.2 a.u. and underestimate the bulk modulus for more than 10%. However, modest size double-zeta plus polarized basis (DZP) basis always offer good results. The largest difference occurs in Ge, where the deviation of lattice constant and bulk modulus between DZP and plane wave basis is 0.07 a.u. and 4 GPa, respectively. After increasing the number of basis to triple-zeta plus double polarized basis (TZDP, we also use notation 3s3p2d), we can see systematically improvement over the DZP orbitals, and are almost identical to those calculated from plane wave basis. The atomic orbitals generated from dimer reference system can also obtain such good results for solid systems, showing remarkable transferability.

The band structures of silicon (diamond structure) are shown in Fig. 4. The lattice

constant is fixed at 10.20 a.u., the energy cutoff is 50 Ry. We compare the band structures calculated by atomic DZP, TZDP and 5ZQP (5s5p4d) bases in Fig. 4(a)(b)(c) respectively and compared with the plane wave results. The black solid lines represent the plane wave results, whereas the blue dotted lines are the results of atomic bases. The Fermi level is fixed at 0 eV. From Fig.4(a) we can see DZP basis already gives very good band structures, for valence bands and the low energy conduction bands, except around L point. The TZDP basis improves the band structures around L point, as illustrated in Fig.4(b), though there is still small difference. If we further increase the basis size to 5ZQP, we can see the energy bands calculated from atomic orbitals are almost identical to those from plane wave basis.

We also calculate the electronic states of a Silicon cluster containing 29 silicon atoms and 38 hydrogen atoms. We calculate lowest 100 states and plot the density of states (DOS). Also we denote 2s1p, 3s2p and 4s3p as DZP, TZDP and QZTP basis for hydrogen, respectively. The results are shown in Fig. 5(a), (b),(c) for the DZP, TZDP and QZTP bases respectively. The DOS calculated by plane wave is shown in black solid line, where as those calculated from atomic orbitals are shown in red dashed lines. For the DZP basis, we find that the DOS of the valence states are almost identical to that calculated from plane wave basis. However, the DOS of conduction electrons shifts to the higher energy side for about 280 meV relative to the plane wave result. The TZDP basis improves the DZP's results, however the DOS of conduction electrons still shifts a little towards the higher energy side. QZTP further improves the results, which are in excellent agreement with those calculated from plane wave basis.

C. GaN, ZnO, Al, MgO, Pb

Now we test our atomic bases for several important materials, including GaN, ZnO, Al and MgO and Pb. GaN, ZnO and Al have several stable structures. Zn has 3d electrons as valence electrons, whereas Al is metallic. They thus offer good examples for comprehensive tests on the quality and transferability of the atomic bases.

GaN has two stable crystal structures, namely, the zinc blende structure (B3) and the wurtzite structure (B4). The energy difference between the two structures is very small. The B3 structure has only one structure parameter, i.e., the lattice constant, whereas the B4 structure can be described by three parameters: the lattice constants a , c and the

internal parameter u , which describes the relative position of the two hexagonal close-packed sublattices. The purpose of the test is to see if the atomic basis set can predict correctly the energy difference between the two structures. The energy cutoff is chosen 120 Ry and the k points is chosen to be $6 \times 6 \times 6$ for B3 and $6 \times 6 \times 4$ for B4. The calculated total energies as functions of volume per atom are shown in Fig. 6, compared to those calculated from plane wave basis. The plane wave calculations indicate that wurtzite structure is more stable than zinc blende structure, which is also predicted correctly from both DZP and TZDP basis sets. We can also see that the total energies are systematically improved from DZP to TZDP. More properties including structure parameters (a , c and u), bulk modulus and the total energies difference between the two structures are shown in Table II. We can see that DZP basis already give very good structure parameters and bulk modulus compared with those calculated from plane wave basis for both B3 and B4 structures. TZDP basis further improves all properties. It gives much better bulk modulus than DZP basis, which reduce the difference from about 10 GPa to less than 1 GPa. The total energy difference between zinc blende structure and the wurtzite structure from plane wave calculations is about 6 meV. Although the energy difference is very small, both DZP and TZDP basis give rather good value, which are 4 meV and 7 meV, respectively. This proves that for GaN, local basis can provide accurate results as good as plane wave basis.

Let us see how the scheme work for systems containing 3d electrons. Zinc is a transition-metal element, which contains 3d electrons. We calculate four structures of ZnO, including rock salt structure (B1), cesium chloride structure (B2), zinc blende structure (B3) and wurtzite structure (B4). The energy cutoff is chosen as 120 Ry, and we use $6 \times 6 \times 6$ k -meshes for B1, B2 and B3 structures and $6 \times 6 \times 4$ k -meshes for B4 structure. We define 2s2p1d for O and 2s1p2d for Zn as DZP basis, whereas 3s3p2d for O and 3s2p3d for Zn, as TZDP basis. The r_{cut} is 8 a.u. for O and 8 a.u. for Zn. We plot total energies vs volume per atom for these four ZnO structures in Fig. 7(b) using DZP basis, compared with the results calculated from plane wave basis shown in Fig. 7(a). Both bases give correct energy order for the four structures compared to experiments.²² As we see the energy diagrams calculated from DZP basis look almost the same as those calculated from plane wave basis, except that all the total energies calculated from DZP basis shift up for about 0.185 eV per atom relative to the plane wave results. The calculations shows that the structures with decreasing energy order is B2, B1, B3 and B4, and ground state structure of ZnO is the wurtzite structure.

Table III further shows the calculated structure parameters, bulk modulus and energy differences of ZnO using DZP and TZDP basis comparing with plane wave results. Both DZP and TZDP basis give accurate lattice constants. The largest difference is less than 0.02 Å compared to plane wave results. However, TZDP basis gives more accurate bulk modulus for all structures. The energy difference between wurtzite phase and zinc blende phase is also calculated accurately using different basis. The energy of structure B4 is 9 meV per atom lower than that of the structure B3 as calculated by plane wave basis. DZP and TZDP give exact the same results. We also show the lattice constant and bulk modulus calculated by Gaussian basis.²² We see that the errors due to pseudopotentials and other approximations are bigger than the errors caused by the atomic bases.

Aluminum is a metal system. It is not obvious that atom-centered atomic basis can describe it well. We test four structures of Aluminum, including the simple cubic (sc) structure, the face-centered cubic (fcc) structure, the body-centered cubic (bcc) structure and the hexagonal-closed packed (hcp) structure. The energy cutoff is fixed at 70 Ry, and the k points are chosen as $6 \times 6 \times 6$. Gaussian smearing is used in all calculations. We use DZP (2s2p1d) orbitals for Aluminum with $r_c=9$ a.u. Figure 8(a), (b) compare the energy diagrams of the Aluminum four structures calculated using plane wave basis and DZP basis. As we see, the atomic basis provide excellent agreement with the plane wave result for all structures. The fcc structure is the lowest-energy structure of Aluminum predicted by both bases. We summarize calculated properties, including lattice constant, bulk modulus and energy difference between different structures of Aluminum in table IV. Surprisingly, we find that DZP basis can provide extremely good results compared to plane wave calculations.¹³ For example, in our calculation, the largest difference of calculated lattice constant is 0.011 Å in bcc structure, whereas the largest difference of bulk modulus is 1 GPa. The DZP basis can also give excellent energy differences between different structures of Aluminum. These results are much better than previous calculations, also using DZP basis.¹³ For example, in Ref. 13, the lattice constants errors for fcc, hcp(a/c) bcc and sc are 0.044 Å 0.054/0.040 Å 0.037 Å 0.013 Å respectively. The bulk modulus errors for fcc, hcp, bcc and sc is 4.9 GPa, 8.5GPa. 5.2 GPa and 2.9 GPa, respectively, which are much larger than those obtained using our bases.

We also test the quality of our atomic bases for some other materials, such as MgO, Pb, etc. The results are summarized in Table V. The energy cutoff is 70 Ry for MgO and 50

Ry for Pb. The k points are $6 \times 6 \times 6$. We all use 2s2p1d for Mg, O, Pb. We use $r_c=8$ a.u. for Mg and O, and $r_c=9$ a.u. for Pb. We compare the results with previous calculations using DZP basis.¹⁰ We find our basis give much better bulk modulus for Pb than previous calculations.

IV. SUMMARY

We propose a unique scheme to construct fully optimized atomic basis sets for density-functional calculations. The shape of the radial functions are optimized by minimizing the *spillage* of the wave functions between the atomic orbital calculations and the converged plane wave calculations for dimer systems. Our method improves upon that of previous methods in three aspects: (i) The shape of atomic orbitals can be generated automatically without any pre-assumptions. (ii) The atomic basis can be systematically improved within the same framework. (iii)The transferability of atomic orbitals bases are improved by carefully choosing the reference systems. The scheme is easy to implement and very flexible. We have done extensive tests of this scheme for wide variety of systems, including semiconductors, ionic, covalent and metallic materials. The results show that the obtained atomic basis sets are very satisfactory for both accuracy and transferability.

Acknowledgments

L.H. acknowledges the support from the Chinese National Fundamental Research Program 2006CB921900, the Innovation funds and “Hundreds of Talents” program from Chinese Academy of Sciences.

-
- ¹ T. Otsuka, T. Miyazaki, T. Ohno, D. R. Bowler, and M. J. Gillan, J. Phys.:Condens. Matter **20**, 294201 (2008).
 - ² V. Blum, R. Gehrke, F. Hanke, P. Havu, V. Havu, X. Ren, K. Reuter, and M. Scheffler, Com. Phy. Commu. **06**, 022 (2009).
 - ³ C.-K. Skylaris, P. D. Haynes, A. A. Mostofi, and M. C. Payne, J. Phys.:Condens. Matter **20**, 064209 (2008).

- ⁴ E. Artacho, E. Anglada, O. Dieguez, J. D. Gale, A. Garcia, J. Junquera, R. M. Martin, P. Ordejon, J. M. Pruneda, D. Sanchez-Portal, et al., *J. Phys.:Condens. Matter* **20**, 064209 (2008).
- ⁵ S. Goedecker, *Rev. Mod. Phys.* **71**, 1085 (1999).
- ⁶ W. Kohn, *Phys. Rev. Lett* **76**, 3168 (1996).
- ⁷ J. M. Soler, E. Artacho, J. D. Gale, A. Garcia, J. Junquera, P. Ordejon, and D. S. Portal, *J. Phys.: Condens. Matter* **14**, 2745 (2002).
- ⁸ T. Ozaki, *Phys. Rev. B* **67**, 155108 (2003).
- ⁹ O. F. Sankey and D. J. Niklewski, *Phys. Rev. B* **40**, 3979 (1989).
- ¹⁰ J. Junquera, O. Paz, D. Sanchez-Portal, and E. Artacho, *Phys. Rev. B* **64**, 235111 (2001).
- ¹¹ D. S. Portal, E. Artacho, and J. M. Soler, *Solid State Communications* **95**, 685 (1995).
- ¹² D. S. Portal, E. Artacho, and J. M. Soler, *J. Phys: Condes Matter* **8**, 3859 (1996).
- ¹³ S. D. Kenny, A. P. Horsfield, and H. Fujitani, *Phys. Rev. B* **62**, 4899 (2000).
- ¹⁴ M. Gusso, *J. Chem. Phys.* **128**, 044102(R) (2008).
- ¹⁵ P. Hohenberg and W. Kohn, *Phys. Rev.* **136**, 864B (1964).
- ¹⁶ W. Kohn and L. J. Sham, *Phys. Rev.* **140**, 1133A (1965).
- ¹⁷ J. P. Perdew and A. Zunger, *Phys. Rev. B* **23**, 5048 (1981).
- ¹⁸ L. Kleinman and D. M. Bylander, *Phys. Rev. Lett* **48**, 1425 (1982).
- ¹⁹ N. Troullier and J. L. Martins, *Phys. Rev. B* **43**, 1993 (1991).
- ²⁰ H. J. Monkhorst and J. D. Pack, *Phys. Rev. B* **13**, 5188 (1976).
- ²¹ E. Anglada, J. M.Soler, J. Junquera, and E. Artacho, *Phys. Rev. B* **66**, 205101 (2002).
- ²² J. Uddin and G. E. Scuseria, *Phys. Rev. B* **74**, 245115 (2006).
- ²³ I. Vurgaftman, J. R. Meyer, and L. R. Ram-Mohan, *Jour. App. Phys* **89**, 5815 (2001).
- ²⁴ C.Kittle, *Introduction to Solid State Physics* (1986).
- ²⁵ Y.-M. Juan and E. Kaxiras, *Phys. Rev. B* **48**, 14944 (1993).
- ²⁶ M. L. Cohen, *Phys. Rev. B* **32**, 7988 (1985).
- ²⁷ K. Karch, J. M. Wagner, and F. Bechstedt, *Phys. Rev. B* **57**, 7043 (1998).

TABLE I: Comparison of the calculated lattice constants a (in a.u.) and bulk modulus B (in GPa) using plane wave basis (PW) and atomic bases for typical III-V and group IV materials.

Compound	a					B				
	SZ	DZP	TZDP	PW	Expr.	SZ	DZP	TZDP	PW	Expr.
GaAs	10.67	10.50	10.49	10.48	10.68 ^a	69	78	77	77	75.57 ^c
GaP	10.28	10.11	10.11	10.10	10.30 ^a	82	92	93	93	89 ^d
GaSb	11.54	11.38	11.37	11.36	11.52 ^a	49	59	58	57	57 ^d
InAs	11.40	11.27	11.28	11.28	11.45 ^a	63	66	65	65	60 ^d
InP	11.07	10.94	10.94	10.93	11.09 ^a	78	79	79	80	71 ^d
InSb	12.33	12.05	12.05	12.07	12.24 ^a	41	50	49	50	47 ^d
AlAs	10.88	10.63	10.62	10.59	10.70 ^a	67	76	76	76	77 ^d
AlP	10.50	10.26	10.25	10.21	10.33 ^a	64	87	88	89	86 ^d
AlSb	11.83	11.58	11.57	11.54	11.59 ^a	48	55	56	56	58 ^d
Ge	10.82	10.68	10.61	10.61	10.70 ^c	57	67	71	71	77.20 ^c
Si	10.59	10.28	10.25	10.23	10.26 ^b	74	94	94	94	99 ^b
C ^e	6.78	6.67	6.67	6.67	6.75 ^b	436	470	467	466	442 ^b

^aI. Vurgaftman, J. R. Meyer and L. R. Ram-Mohan, Ref. 23.

^bC. Kittel, Ref. 24.

^cYu-Min Juan and Efthimios Kaxiras, Ref.25.

^dMarvin L. Cohen, Ref.26.

^eEnergy cutoff 100 Ry is used.

TABLE II: Basis comparison for GaN Zinc blende (B3) and wurtzite (B4) structures. a , c (in Å) are the lattice constants, and c (in Å) is the internal parameter. B (in GPa) is the bulk modulus, whereas ΔE (in eV/atom) is the total energy difference between different structures. The energy difference is set to zero for B4 structure. The data of “Other calculations” and experimental values are taken from the reference 27.

Compound	Properties	PW	DZP	TZDP	Other calculations	Experiment
GaN(B3)	a	4.424	4.441	4.422	4.446~4.46	4.49
	B	207	197	208	184~207	173
	ΔE	0.006	0.004	0.007		
GaN(B4)	a	3.130	3.142	3.130	3.126~3.170	3.160~3.189
	c/a	1.629	1.631	1.630	1.620~1.638	1.621~1.626
	u	0.377	0.377	0.377	0.377~0.379	
	B	207	194	207	190~245	188~237
	ΔE	0	0	0		

TABLE III: Basis comparison for ZnO rock salt (B1), cesium chloride (B2), zinc blende (B3) and wurtzite (B4) structures. a , c (in Å) are the lattice constants, and c (in Å) is the internal parameter. B (in GPa) is the bulk modulus, whereas ΔE (in eV/atom) is the total energy difference between different structures. The energy difference is set to zero for B4 structure. The results from Gaussian orbitals and the experimental values are taken from Ref. 22.

Compound	Properties	PW	DZP	TZDP	Gaussian	Experiment
ZnO(B1)	a	4.286	4.296	4.296	4.218	4.271-4.283
	B	196	198	195	203	177-228
	ΔE	0.068	0.066	0.058		
ZnO(B2)	a	2.653	2.659	2.658	2.614	
	B	194	190	191	201	
	ΔE	0.639	0.647	0.620		
ZnO(B3)	a	4.583	4.596	4.595	4.509	4.62
	B	152	150	151	154	
	ΔE	0.009	0.009	0.009		
ZnO(B4)	a	3.256	3.266	3.264	3.205	3.248-3.250
	c	5.246	5.256	5.255	5.151	5.207-5.210
	u	0.381	0.381	0.381	0.381	0.382
	B	152	150	151	155	136-183
	ΔE	0	0	0		

TABLE IV: Comparison of the calculated lattice constants a , c (in Å), bulk modulus B (in GPa) and energy difference ΔE (in eV/atom) for Aluminum fcc, bcc, sc and hcp structures, using different basis. The energy difference is set to zero for fcc structure. The results of “Other DZP” and “Other PW” are taken from Ref. 13.

Compound Properties		PW	DZP	Other DZP	Other PW
Al(fcc)	a	3.964	3.974	4.011	3.967
	B	80	79	76.2	81.1
	ΔE	0	0	0	0
Al(bcc)	a	3.175	3.186	3.212	3.175
	B	75	75	67.1	72.3
	ΔE	0.1167	0.1157	0.128	0.121
Al(sc)	a	2.678	2.678	2.688	2.675
	B	54	54	57.9	60.8
	ΔE	0.5819	0.6018	0.479	0.483
Al(hcp)	a	2.806	2.805	2.846	2.793
	c	1.638	1.639	1.63	1.67
	B	82	83	71.6	80.1
	ΔE	0.0836	0.0821	0.032	0.038

TABLE V: Comparison of the calculated lattice constants a (\AA) and bulk modulus B (GPa) using atomic orbitals to those from plane wave calculations for MgO and Pb. The data of “Other DZP”, “Other PW” and experimental values are taken from Ref. 10.

Compound	Properties	PW	DZP	Other DZP	Other PW	Experiments
MgO(B1)	a	4.233	4.238	4.11	4.10	4.21
	B	169	169	167	168	152
Pb(fcc)	a	4.873	4.875	4.88	4.88	4.95
	B	56	55	64	54	43

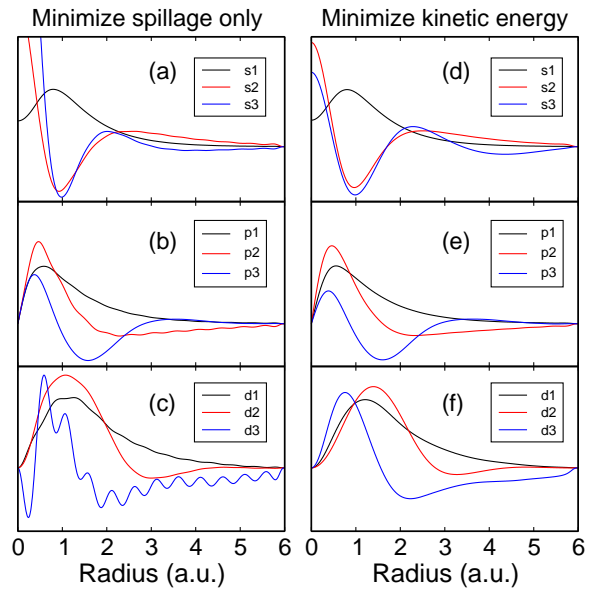


FIG. 1: (Color online) (a), (b), (c) The radial functions of unoptimized carbon s , p , d orbitals respectively. (d), (e), (f) The radial functions of optimized carbon s , p , d orbitals.

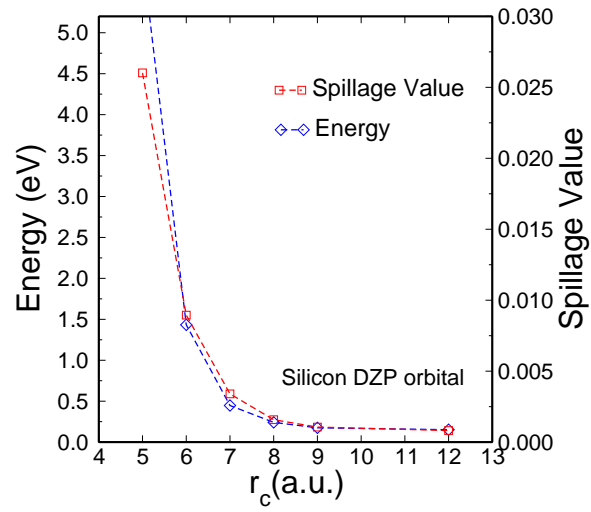


FIG. 2: (Color online) The total energy difference (blue line) and average spillage value of five dimers (red line) as functions of orbital radius cutoff r_c for Si DZP orbitals.

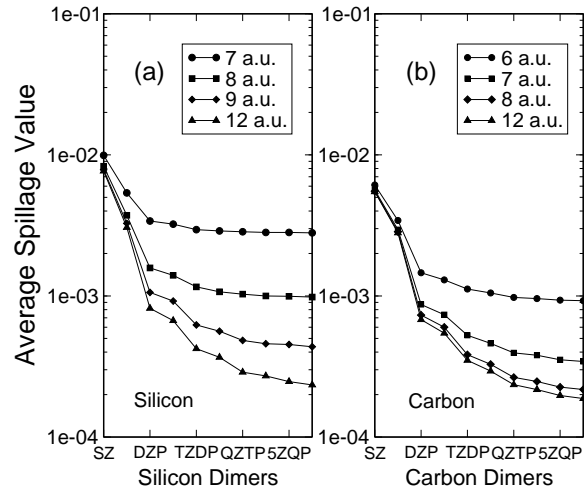


FIG. 3: Convergence of spillage value as functions of orbital radius cutoff r_c and basis size for (a) Si and (b) Carbon dimers.

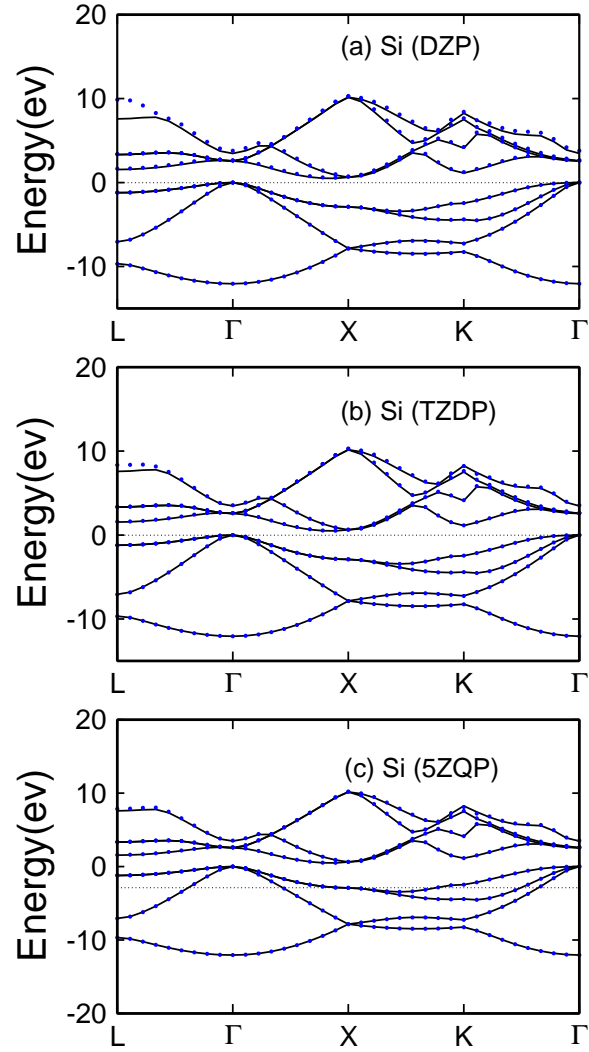


FIG. 4: (Color online) Comparison of the band structures of Si calculated by different atomic bases (blue dotted lines) and plane wave basis (solid black lines).

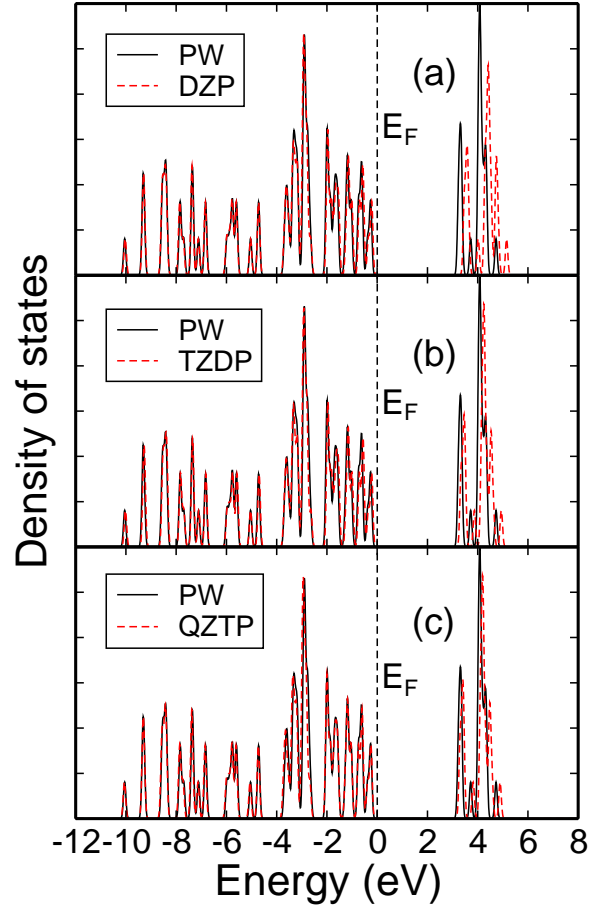


FIG. 5: (Color online) Comparison of the density of states (DOS) of $\text{Si}_{29}\text{H}_{38}$ cluster calculated by different atomic bases and plane wave basis.

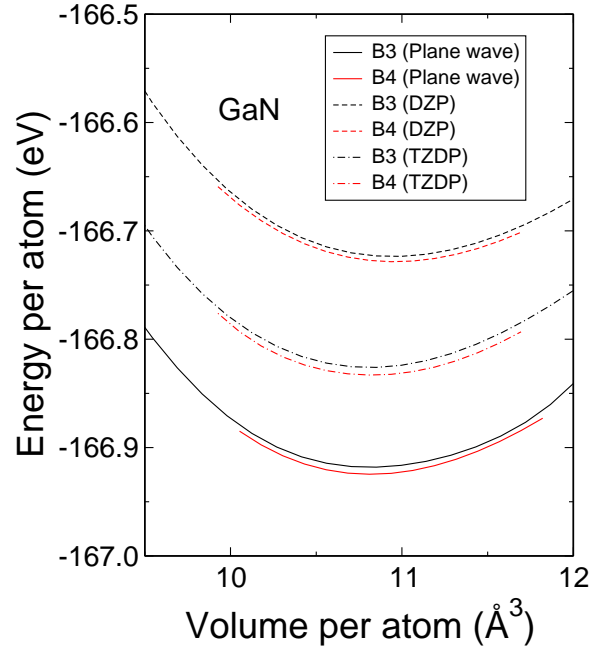


FIG. 6: (Color online) Comparison of the total energies of GaN zinc blende structure (B3) and the wurtzite structure (B4) as functions of volume per atom using different atomic bases to those using plane wave basis.

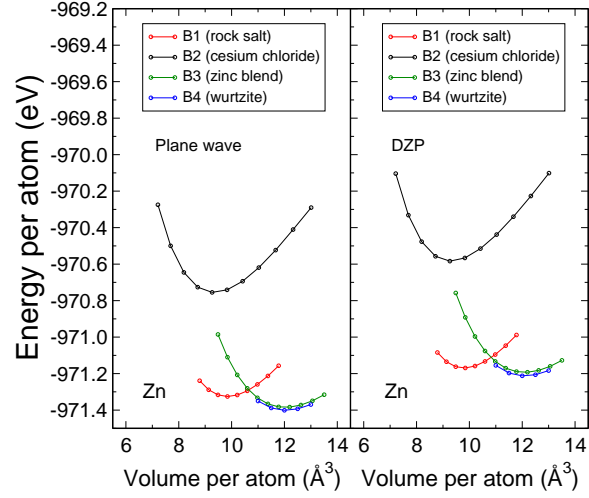


FIG. 7: (Color online) Comparison of the total energies of ZnO rock salt structure (B1), cesium chloride structure (B2), zinc blende structure (B3) and wurtzite structure (B4) as functions volume per atom (a) using plane wave basis to (b) those using atomic DZP basis.

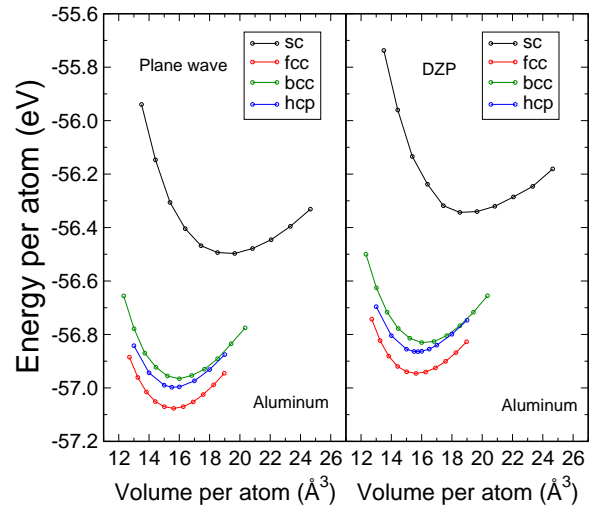


FIG. 8: (Color online) Comparison of the total energies of Al sc, fcc, bcc, hcp structures as functions of volume per atom (a) using plane wave basis to (b) those using atomic DZP basis.